Variable Power and Rate Allocation Using Simple CQI for Multiuser OFDMA-CDM Systems

Kwang Soon Kim, *Senior Member, IEEE*, and Yun Hee Kim, *Senior Member, IEEE*

***Abstract*—This paper presents variable power and rate allocation (PRA) for a multiuser orthogonal frequency division multiple access code division multiplexing (OFDMA-CDM) system which exploits both orthogonality among users and symbol-level diversity. To predict the link performance, we analyze the post-processing SNR as the transmit power (TP) varies when the minimum mean square error combiner (MMSEC) is employed. It is shown from analysis that the MMSEC SNR is nonlinear in TP, but is bounded by the harmonic and the arithmetic means of the subcarrier SNRs. From the observation, we propose two variable PRA methods using a simple channel quality indication and a required TP estimation method. Simulation results show that the proposed methods not only guarantee the target performance but also increase the throughput at the same or slightly increased feedback overhead compared with the fixed TP allocation case.**

***Index Terms*—OFDMA, code division multiplexing, link adaptation, power and rate allocation, MMSE receiver.**

I. Introduction

NEXT generation wireless networks require high spectral efficiency to support various multimedia services at a lower cost. To meet such requirements, they adopt multiple access schemes based on orthogonal frequency division multiplexing (OFDM) favorable to high-rate data transmission [1]–[5]. Among the schemes, multicarrier code division multiple access (MC-CDMA) [1] and orthogonal frequency division multiple access (OFDMA) [2]–[5] are most popular. From the performance aspect, OFDMA with user, bit, and power adaptation in the frequency domain would be preferred [6], [7]. However, such an adaptation in the frequency domain requires a large amount of feedback, which makes the channel variation tracking difficult in mobile applications. To reduce the feedback overhead, it is often preferred to allow frequency diversity in each subchannel (SCH) and to perform a SCH-wise link adaptation.

Code division multiplexing (CDM) as in MC-CDMA [8] is one typical method allowing frequency diversity in the SCH. The diversity mode of OFDMA (called OFDMA in the sequel) also exploits frequency diversity in the SCH through channel coding [3], [9], [10]. In the single user case, MC-CDMA exploiting symbol-level diversity could provide a lower bit error rate (BER) than OFDMA [8] and could predict the link performance for adaptive transmission with a more simple channel quality indication (CQI) [11]. In the multiuser case, MC-CDMA suffers from inter-user interference which makes link performance prediction difficult. The interference problem can be resolved with OFDMA-CDM which separates users with orthogonal SCHs and code-multiplexes the data symbols of the same user in the SCH. Despite the fact, there seems to be no literature applying variable power and rate allocation (PRA) to OFDMA-CDM while a performance gain is observed in a recent work by applying variable PRA to OFDMA [10].

In this paper, we consider multiuser variable PRA for a single-input single-output (SISO) OFDMA-CDM system when the receiver employs the minimum mean square error combiner (MMSEC) [12]. To predict the link performance in the variable power case, we analyze the signal-to-noise power ratio (SNR) at the MMSEC as the transmit power (TP) varies. The analysis shows that the MMSEC SNR is nonlinear in TP, which makes the required TP estimation using a typical linear interpolation not always guarantee the target packet error rate (PER). Based on the observation that the MMSEC SNR is bounded by the arithmetic and the harmonic means of the subcarrier SNRs, we propose two variable PRA methods estimating the required TP with a simple CQI[1] meeting the target PER. The benefit of the proposed methods will be shown by evaluating the throughput and the actual PER.

The remaining of the paper is organized as follows. Section II describes an adaptive OFDMA-CDM system using low-density parity-check (LDPC) codes [9], [10] and quadrature amplitude modulation (QAM). From the analysis on the MMSEC SNR in Section III, we propose two PRA methods meeting the target performance in Section IV. Simulation results are provided in Section V, followed by conclusions in Section VI.

II. System Model

Consider the downlink of a cellular system, where a frame consists of N_t OFDM symbols each with K_f subcarriers. The frame is orthogonally divided into a pilot SCH and D data SCHs as shown in Fig. **??**, which is similar to the diversity mode of IEEE 802.16e [3]. In each OFDM symbol, F_p subcarriers are allocated to the pilot SCH while F subcarriers are allocated to a data SCH with $F = (K_f - F_p)/D$. Thus, the pilot SCH consists of L_p $(= N_t \times F_p)$ resources while each data SCH consists of L $(= N_t \times F)$ resources, well distributed in the time domain and the frequency domain. In this paper, a data SCH is assigned to only a single user as in IEEE 802.16e

[1]The CQI is simple in that it can be represented with only a small amount of bits when compared with full channel state information (CSI).

Manuscript received March 26, 2008; revised July 26, 2008, October 11, 2008, and January 9, 2009; accepted February 21, 2009. The associate editor coordinating the review of this letter and approving it for publication was H. Chen.

K. S. Kim is with the Dept. of Electrical and Electronic Engineering, Yonsei University, Seoul 120-749, Korea (e-mail: ks.kim@yonsei.ac.kr).

Y. H. Kim is with the Dept. of Electronics and Radio Engineering, Kyung Hee University, Yongin, Gyeonggi 446-701, Korea (e-mail: yheekim@khu.ac.kr).

This work was supported by the MKE, Korea, under the ITRC support program supervised by the IITA (IITA-2009-C1090-0902-0010).

Digital Object Identifier 10.1109/TWC.2009.080413

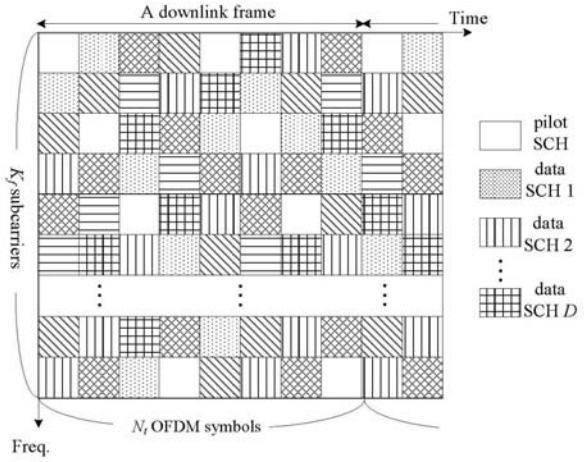

(a) Frame structure.

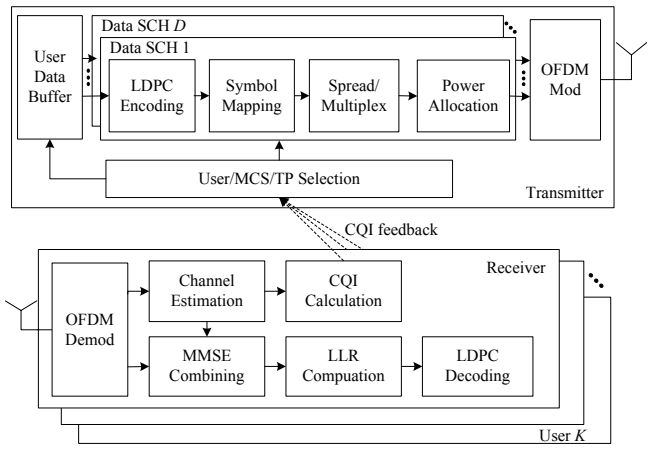

(b) Transceiver model.

Fig. 1. System model.

while the data symbols of the *same* user are code-multiplexed when transmitted over the data SCH. It should be also noted that OFDMA-CDM has no inter-user interference unlike MC-CDMA which code-multiplexes data symbols of *different* users [8].

Fig. 1(b) shows the system model of SISO OFDMA-CDM constructing a modulation and coding scheme (MCS) set with LDPC codes and QAM. The required SNR table of the MCS set is pre-determined and stored at the base station (BS). Each user reports its CQI to the BS for variable PRA. Based on the CQI and the SNR table, the user/MCS/TP selector selects D active users from K users and determines the MCS and TP of each active user. The information blocks of active users are then processed through LDPC encoding and symbol mapping.

Let $\{s_{k,l}, l = 1, 2, \cdots, L\}$ denote the QAM symbols of the kth user with $E\{|s_{k,l}|^2\} = 1$. The QAM symbols are arranged as $\mathbf{s}_{k,n} = [s_{k,(n-1)F+1}\ s_{k,(n-1)F+2}\ \cdots\ s_{k,nF}]^T$ to be transmitted over the nth OFDM symbol. The symbol vector $\mathbf{s}_{k,n}$ is then spread, multiplexed, and scaled by the allocated TP P_k to output $\mathbf{x}_{k,n} = \sqrt{P_k}\mathbf{C}\mathbf{s}_{k,n}$. Here, $\mathbf{C} = [c_{i,j}]$ is an $F \times F$ code matrix satisfying $\mathbf{C}\mathbf{C}^\dagger = \mathbf{C}^\dagger\mathbf{C} = \mathbf{I}_F$, where $\dagger$ is Hermitian and $\mathbf{I}_F$ is the identity matrix of size F. Hence, CDM is separately performed in each data SCH over F data symbols to be mapped onto an OFDM symbol. At the same time, pilot symbols are generated with a fixed TP P_{pi}. Both pilot and CDM symbols are then mapped to their SCHs and transmitted after OFDM modulation.

At the receiver, the received symbols in the frequency domain are obtained through OFDM demodulation. They are arranged in the vector $\mathbf{r}_{k,n}$ corresponding to $\mathbf{s}_{k,n}$ as

$$\mathbf{r}_{k,n} = \sqrt{P_k}\mathbf{H}_{k,n}\mathbf{C}\mathbf{s}_{k,n} + \mathbf{w}_{k,n}. \tag{1}$$

In (1), $\mathbf{H}_{k,n} = \mathrm{diag}(h_{k,n,1}, \ldots, h_{k,n,F})$ is the diagonal matrix representing the channel frequency response (CFR) and $\mathbf{w}_{k,n}$ is the zero-mean AWGN vector with covariance matrix $\sigma_0^2\mathbf{I}_F$. Through equalization and despreading, the symbol vector is estimated as $\hat{\mathbf{s}}_{k,n} = \mathbf{C}^\dagger\mathbf{G}_{k,n}\mathbf{r}_{k,n}$, where the equalization matrix is given by

$$\mathbf{G}_{k,n} = \sqrt{P_k}\mathbf{H}_{k,n}^\dagger(P_k\mathbf{H}_{k,n}\mathbf{C}\mathbf{C}^\dagger\mathbf{H}_{k,n}^\dagger + \sigma_0^2\mathbf{I}_F)^{-1}. \tag{2}$$

With full code multiplexing using orthogonal codes ($\mathbf{C}\mathbf{C}^\dagger = \mathbf{I}_F$), $\mathbf{G}_{k,n}$ becomes diagonal with $g_{k,n,l} = \sqrt{P_k}h_{k,n,l}^*/(P_k|h_{k,n,l}|^2 + \sigma_0^2)$ for the lth diagonal element [12]. The log-likelihood ratios are then computed with $\hat{\mathbf{s}}_{k,n}$ for LDPC decoding. In addition, the CQI is calculated with the channel estimates and is reported to the BS.

III. Analysis on MMSEC SNR with Variable TP

To derive an appropriate CQI and a TP estimation method, we analyze the SNR of $\hat{\mathbf{s}}_{k,n}$ (called MMSEC SNR in the sequel) which determines the link performance. When the TP is P_k, the MMSEC SNR is derived as [13]

$$\beta_{k,n}(P_k) = \frac{\eta_{k,n}(P_k)}{1 - \eta_{k,n}(P_k)}, \tag{3}$$

where

$$\begin{aligned}\eta_{k,n}(P_k) &= \frac{1}{F}tr\left\{\sqrt{P_k}\mathbf{G}_{k,n}\mathbf{H}_{k,n}\right\} \\ &= \frac{1}{F}\sum_{l=1}^{F}\frac{\gamma_{k,n,l}(P_k)}{1+\gamma_{k,n,l}(P_k)}.\end{aligned} \tag{4}$$

In (4), $tr\{\cdot\}$ denotes the trace and $\gamma_{k,n,l}(P_k) = |h_{k,n,l}|^2P_k/\sigma_0^2$ is the subcarrier SNR. If the time variation of the channel is negligible in the SCH and F is large enough to obtain the full frequency diversity, the MMSEC SNR becomes similar for all n as $\beta_k(P_k) \cong \beta_{k,n}(P_k)$. Thus, the BS can predict the link performance of OFDMA-CDM when $\beta_k(P_k)$ is known.

On the other hand, the receiver cannot provide the MMSEC SNR $\beta_k(P_k)$ at the allocated TP P_k since P_k is not known before transmission. The receiver instead feedbacks the CQI $\mathcal{B}_k$ evaluated at some TP P_{ref} and the BS estimates $\beta_k(P_k)$ at another P_k. To derive an adequate estimation method, we now investigate how $\beta_k(P_k)$ varies with P_k. For notational simplicity, we ignore user index k in the variables of (3) and (4) as $\beta(P)$, $\eta(P)$ and $\gamma_l(P)$. The following two theorems then summarize the properties of $\beta(P)$ with respect to P. The proofs of the theorems are provided in Appendix.

Theorem *1:* The MMSEC SNR $\beta(P)$ is nonlinear in P such that

$$\beta(P) \geq \frac{P}{P_{ref}}\beta(P_{ref}) \quad \text{if } P \leq P_{ref} \tag{5}$$

and

$$\beta(P) < \frac{P}{P_{ref}}\beta(P_{ref}) \quad \text{if } \quad P > P_{ref} \tag{6}$$

for some reference TP P_{ref}.

Theorem *2:* The MMSEC SNR $\beta(P)$ is bounded by the arithmetic mean $m(P)$ and the harmonic mean $\tilde{m}(P)$ of subcarrier SNRs $\{\gamma_l(P)\}_{l=1}^{F}$ as

$$\tilde{m}(P) \leq \beta(P) \leq m(P), \tag{7}$$

with $\beta(P) \to m(P)$ if $P \to 0$ and $\beta(P) \to \tilde{m}(P)$ if $P \to \infty$.

Fig. 2 shows $\beta(P)$, $m(P)$, and $\tilde{m}(P)$ in dB obtained with a given CFR matrix $\mathbf{H}_{k,n}$. Indeed, i) $\beta(P)$ is nonlinear in P and ii) bounded by $m(P)$ and $\tilde{m}(P)$ which are linear in P. It is also noted that the estimation of $\beta(P)$ by linear interpolation $\bar{\beta}(P) = \frac{P}{P_{ref}}\beta(P_{ref})$ from $\beta(P_{ref})$ is smaller than the actual $\beta(P)$ if $P \leq P_{ref}$ and is larger than the actual $\beta(P)$ if $P > P_{ref}$. It implies that we cannot always guarantee the target PER if a user reports the CQI $\beta(P_{pi})$ obtained with pilot symbols and the BS utilizes $\bar{\beta}(P)$ linearly interpolated from the CQI as in a usual way.

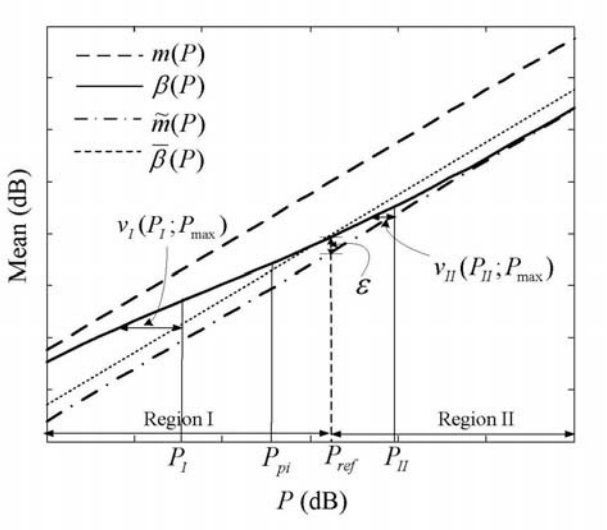

Fig. 2. Means of the instantaneous SNRs as TP P varies.

IV. Variable Power and Rate Allocation

In this section, we propose multiuser variable PRA methods using proper required TP estimation to meet the target PER performance.

A. Required TP Estimation with CQI

As one method estimating the required TP, we propose the piecewise linear interpolation (PLI) in the two regions (I and II) shown in Fig. 2. In the PLI, the kth user feedbacks the CQI $\{\zeta_k, \epsilon_k\}$ obtained at some TP $P_{ref} = \rho P_{avg}$, where $\zeta_k = \beta_k(P_{ref})$, $\epsilon_k = \beta_k(P_{ref})/\tilde{m}_k(P_{ref})$, and P_{avg} is the average TP. The CQI is computed by scaling the received SNR $\{\gamma_{k,l}(P_{pi})\}$ of the pilot symbols transmitted at TP P_{pi}: $\beta_k(P_{ref})$ and $\tilde{m}_k(P_{ref})$ are computed with the scaled SNRs $\gamma_{k,l}(P_{ref}) = \frac{P_{ref}}{P_{pi}}\gamma_{k,l}(P_{pi})$. Here, P_{ref} is assumed to be predetermined and is informed to all users. With $\{\zeta_k, \epsilon_k\}$, the BS estimates $\beta_k(P_k)$ with $\hat{\beta}_k(P_k) = \zeta_k \frac{P_k}{P_{ref}}$ if $P_k \leq P_{ref}$ (region I) and with $\hat{\beta}_k(P_k) = \frac{\zeta_k}{\epsilon_k}\frac{P_k}{P_{ref}}$ if $P_k > P_{ref}$ (region II). Actually, $\hat{\beta}_k(P_k)$ in the region II is equivalent to the linear interpolation of $\tilde{m}_k(P_{ref})$. Here, we use ϵ_k for CQI instead of $\tilde{m}_k(P_{ref})$ to reduce the number of feedback bits.

Let $SNR_w^{(j)}$ denote the minimum SNR meeting the target PER when the jth MCS is used in the AWGN channel. The minimum TP $P_k^{(j)}$ required to allocate the jth MCS to the kth user should satisfy $\hat{\beta}_k(P_k^{(j)}) = SNR_w^{(j)}$. Hence, the required TP for the jth MCS is estimated in the PLI as

$$P_k^{(j)}[dB] = \begin{cases} P_{ref}[dB] + SNR_w^{(j)}[dB] - \zeta_k[dB], & \text{if } P_k^{(j)} \leq P_{ref} \\ P_{ref}[dB] + SNR_w^{(j)}[dB] - \zeta_k[dB] + \epsilon_k[dB], & \text{otherwise} \end{cases} \tag{8}$$

where $[dB]$ denotes the value in dB. The TP estimated by (8) always guarantees the target PER since it is always larger than the actually required TP by $v_I(P_k^{(j)}; P_{ref})$ in the region I and $v_{II}(P_k^{(j)}; P_{ref})$ in the region II as shown in Fig. 2. In the method, P_{ref} should be chosen near to P_{avg} to balance the tradeoff between power losses v_I and v_{II} in the two regions.

To avoid the feedback of ϵ_k in the PLI, we propose another TP estimation called bounded linear interpolation (BLI). In the BLI, TP is limited as $P_k^{(j)} \leq P_{ref}$ (region I). The required TP estimation for the BLI is the same with that for the PLI in the region I using the CQI $\{\zeta_k\}$. In the BLI, P_{ref} should be also chosen appropriately considering the dynamic range of TP and the power loss v_I in the region I.

B. Iterative PRA Algorithm

With $P_k^{(j)}$ estimated, the BS selects D active users and their MCS and the final TP for transmission over D data SCHs. The selection is performed to maximize the throughput when total available TP per OFDM symbol is P_t: if $r^{(j)}$ is the data rate of the jth MCS, a user $k^*(d)$ and its MCS $j_{k^*(d)}$ and TP $P_{k^*(d)}^{(j_{k^*(d)})}$ for the dth data SCH are selected as follows.

$$\left\{k^*(d), j_{k^*(d)}, P_{k^*(d)}^{(j_{k^*(d)})}\right\} = \arg \max_{\{k(d), j_{k(d)}\}} \sum_{d=1}^{D} r^{(j_{k(d)})},$$
$$\text{subject to } \sum_{d=1}^{D} P_{k(d)}^{(j_{k(d)})} \leq P_t - P_{pi}. \tag{9}$$

Due to the complexity in solving (9), we apply a suboptimal approach separating user selection from PRA as in [10]. The method first selects D active users maximizing the

throughput when the TP is the same as $P_{avg} = (P_t - P_{pi})/D$. With the selected D users, we perform the iterative PRA of [10]. At each iteration of the iterative PRA, the remaining power is calculated as $P_r = P_t - P_{pi} - \sum_{d=1}^{D} P_{k(d)}^{(j_{k(d)})}$. At the same time, the required amount $P^+(d)$ of the additional power (the required amount $P^-(d)$ of the saved power) for increasing (decreasing) MCS $j_{k(d)}$ of the user assigned to the dth data SCH is calculated for the active user set. Then the remaining power is allocated to the users of which the data rates can be increased with a smaller amount of additional power. If the BLI is used for TP estimation, the additional condition, $P_{k(d)}^{(j_{k(d)})} \leq P_{ref}$, is included in the iterative PRA. Although the exact complexity analysis of the iterative PRA algorithm is not the main interest of this paper, we would like to note that it can be considered as a coded version of the bit loading algorithm with similar complexity and can be easily implemented in software at the BS.

With the PRA presented here, an analytical derivation of the optimal value of P_{ref} is hardly tractable since it depends on the fading statistics, the numbers of users and data SCHs, and the MCS set applied. To provide some intuition on how to select P_{ref}, we may instead consider an asymptotic case, where K and D are sufficiently large and the discrete-valued data rate of the MCS set is replaced by the continuous-valued channel capacity. For the case, a suboptimal P_{ref}^* (i.e., ρ^*) is obtained by choosing the smallest value with which the performance loss caused by the power limit is unnoticeable by minimizing the power loss in the region I at some negligible power loss in the region II. Then, the power allocation using the BLI becomes equivalent to the single user water-filling problem in a fading channel with a peak power constraint ($P_k \leq P_{ref}$) [14] and the performance loss due to the peak power constraint can be easily evaluated. In addition, P_{ref}^* obtained for the BLI can be also applied in the PLI since it can also balance the power loss in the regions I and II.

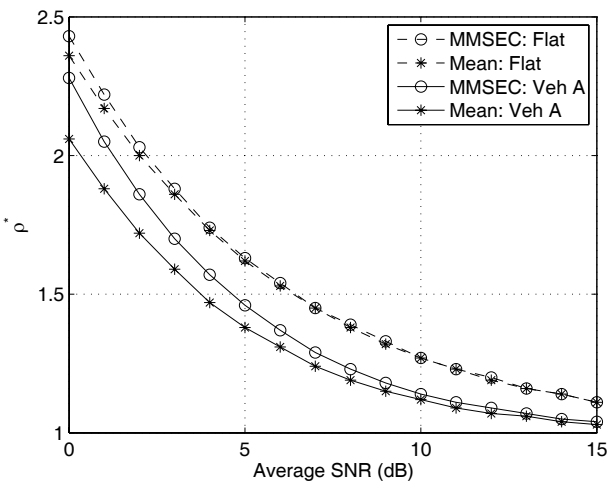

Fig. 3. Required ρ^* obtained from the water-filling algorithm under the peak power constraint.

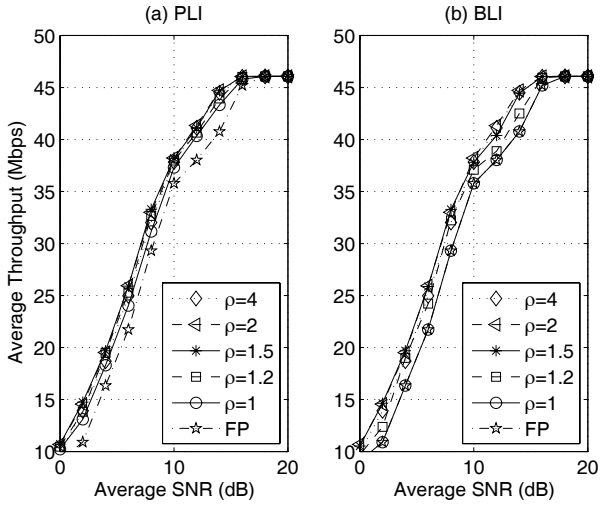

Fig. 4. Average throughput of OFDMA-CDM with variable PRA when various ρ is applied to TP estimation with $K = 60$: (a) PLI. (b) BLI.

V. Simulation Results

We evaluate the performance of the OFDMA-CDM with variable PRA using the system parameters of the HMm test-bed developed by ETRI, Korea, for 4G mobile systems [2], [9]: the system bandwidth is 20 MHz, the FFT size is 2048, and the OFDM data duration is 100 μs. The frame parameters are given by $N_t = 8$, $K_f = 1756$, $F_p = 220$, $L_p = 2200$, $D = 12$, $F = 128$, and $L = 1024$. In the MCS set, there are 9 schemes constructed by QPSK, 16-QAM, and 64-QAM combined with some code rate between $1/6$ and $5/6$. The data rates $\{r^{(j)}\}$ of MCSs are 0, 0.384, 0.768, 1.536, 2.304, 3.072, 3.840, 4.608, and 5.376 Mbps and the required SNRs $\{SNR_w^{(j)}\}$ meeting the target PER of 10^{-2} are obtained as $-\infty$, -2.8, 0.1, 4.1, 7.1, 8.7, 12.5, 13.8, and 16.8 dB. In Figs. 4-6, we set the number K of users to be 60 and apply the ITU-R vehicular (Veh) A channel composed of 6 resolvable Rayleigh fading paths [15].

Before evaluating the system performance, we obtain a proper range of P_{ref} by searching for ρ^* through the water-filling algorithm under the peak power constraint. Fig. 3 shows ρ^* for the average SNR when the instantaneous SNR determining the capacity is given by the MMSEC SNR for our system. We consider both the frequency-*flat* Rayleigh fading channel and the frequency-selective *Veh A* channel to observe the effect of different fading statistics. We also compare the case when the SNR is given by the arithmetic mean to observe the effect of the SNR type. It is observed that ρ^* depends not only on the average SNR and but also on the distribution model of the SNR characterized by the multipath delay model and the SNR type employed. Here, ρ^* is more significantly affected by the average SNR than the distribution model of the SNR. To make the performance loss negligible over the SNR range of our interest, it would be appropriate to have $\rho \approx 2$.

To confirm the value of ρ^* obtained in Fig. 3, we evaluate the average throughput of the OFDMA-CDM with variable PRA for various ρ in Fig. 4. For the PLI and BLI, $\rho = 1.5$ and 2 are appropriate as expected in Fig. 3 by balancing the power loss tradeoffs in the regions I and II. Compared with the maximum throughput achieved, the BLI with $\rho = 1$ suffers

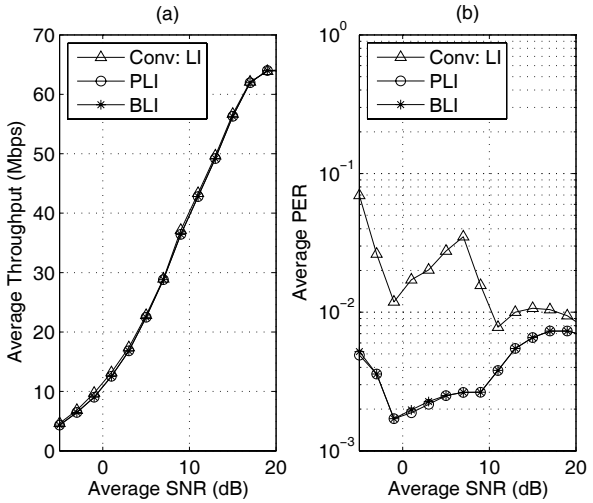

Fig. 5. Average throughput of OFDMA-CDM with variable PRA when different TP estimation methods are applied with $K = 60$: (a) Throughput (b) PER

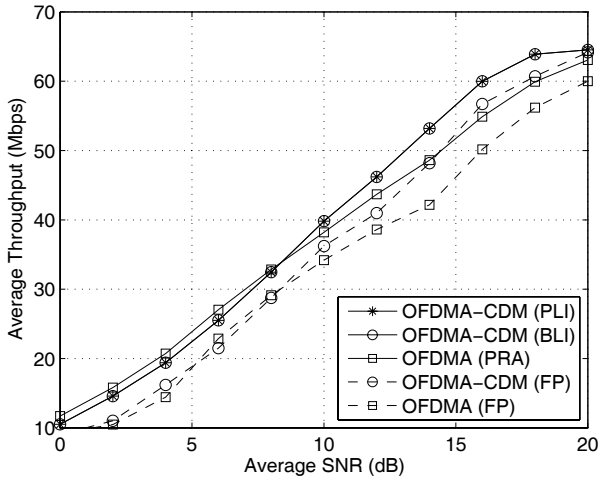

Fig. 6. Performance comparison of OFDMA-CDM and OFDMA when variable PRA methods are applied with $K = 60$.

from a significant loss in throughput by limiting the TP up to $P_{ref} = P_{avg}$. The PLI with $\rho = 1$ also experiences some performance degradation due to the power loss in the region II but the loss is smaller than the BLI case. A slight throughput loss is also observed with $\rho = 4$ by using more TP than required in the region I. In essence, the proposed variable PRA methods with an appropriate value of ρ provide about $1.5 \sim 2$ dB SNR gain over the FP case.

Fig. 5 compares the throughput and the PER when the proposed PLI and BLI with $\rho = 2$ and the conventional method using linear interpolation (LI) are applied for variable PRA in the OFDMA-CDM. It is shown that the three estimation methods provide almost the same performance in throughput. However, the conventional method fails in meeting the target PER while the proposed methods always guarantee the target PER. A larger PER of the conventional method is due to the underestimation of the required TP in the region II by ignoring the non-linearity of the MMSEC SNR. It is also observed that the BLI and the PLI exhibit almost same performance in both throughput and PER with a proper choice of ρ. Thus, the BLI requiring less feedback overhead would be preferable to support the services with tight constraints on the delay and the packet loss probability. The throughput of the OFDMA-CDM is also compared with that of OFDMA in Fig. 6 when similar variable PRA methods [10][2] are employed. The results show that OFDMA-CDM outperforms OFDMA in the mid to high SNR region, i.e., from 8 to 20 dB, at the less feedback overhead.

We also would like to note that the limit on the CQI size would degrade the performance. However, the degradation is not significant in practice if 5 (or 6) bits are allowed for CQI as in the currently deployed systems. For example, the quantization error is at most 0.5 (or 0.25) dB if the SNR range of interest is from -5 dB to 27 dB and a uniform quantization is applied.

[2]The OFDMA system utilizes the arithmetic mean and the normalized standard deviation of the subcarrier SNRs for CQI. The required TP is estimated with linear interpolation of CQI due to the linearity of CQI in TP.

VI. Conclusion

In this paper, we considered variable power and rate allocation (PRA) for multiuser OFDMA-CDM systems. We analyzed the MMSEC SNR for variable TP and showed that the MMSEC SNR is nonlinear in TP, but is bounded by the arithmetic and the harmonic means of the subcarrier SNRs. To guarantee the target PER despite the non-linearity of the MMSEC SNR, we proposed two variable PRA methods using PLI and BLI for required TP estimation, which utilize some simple CQI feedback obtained at an appropriate reference TP. Simulation results showed that the proposed variable PRA methods provide 1.5 dB $\sim$ 2 dB SNR gain over the fixed power allocation case. In addition, it was observed that the proposed methods using PLI and BLI meet the target PER performance while the conventional method using linear interpolation fails. This feature makes the proposed methods more attractive to the services with tight constraints on the delay and the packet loss probability. Furthermore, it was also observed that the OFDMA-CDM with variable PRA using PLI outperforms the OFDMA counterpart in the mid to high SNR region at a smaller feedback overhead. Thus, the OFDMA-CDM with variable PRA could be an appropriate choice for a cellular network when the feedback overhead is allowed to be at most comparable to that of the currently deployed single-carrier systems.

Appendix A
Proof of Theorem 1

Applying $\gamma_i(P_{ref}) = \frac{P_{ref}}{P}\gamma_i(P)$, we have

$$\begin{aligned}\beta(P)-\frac{P}{P_{ref}}\beta(P_{ref}) &= \frac{\sum_{i=1}^{F}\frac{\gamma_i(P)}{1+\gamma_i(P)}}{\sum_{i=1}^{F}\frac{1}{1+\gamma_i(P)}}-\frac{P}{P_{ref}}\frac{\sum_{j=1}^{F}\frac{\gamma_j(P_{ref})}{1+\gamma_j(P_{ref})}}{\sum_{j=1}^{F}\frac{1}{1+\gamma_j(P_{ref})}}\\ &= \frac{\sum_{i=1}^{F}\frac{\gamma_i(P)}{1+\gamma_i(P)}}{\sum_{i=1}^{F}\frac{1}{1+\gamma_i(P)}}-\frac{\frac{1}{\theta}\sum_{j=1}^{F}\frac{\theta\gamma_j(P)}{1+\theta\gamma_j(P)}}{\sum_{j=1}^{F}\frac{1}{1+\theta\gamma_j(P)}}\\ &= \frac{\sum_{i=1}^{F}\sum_{j=1}^{F}A_{i,j}}{\sum_{i=1}^{F}\sum_{j=1}^{F}\frac{1}{(1+\gamma_i(P))(1+\theta\gamma_j(P))}},\end{aligned} \tag{10}$$

where $\theta = P_{ref}/P$ and $A_{i,j} = \frac{\gamma_i(P)-\gamma_j(P)}{(1+\gamma_i(P))(1+\theta\gamma_j(P))}$. The numerator in (10) can be divided into three sums, $S_1 = \sum_{j=i} A_{i,j}$, $S_2 = \sum_{j>i} A_{i,j}$, and $S_3 = \sum_{i>j} A_{i,j}$. Firstly, $S_1 = 0$ since $A_{i,i} = 0$. Secondly, $S_2 = \sum_{i=1}^{F}\sum_{j=i+1}^{F} A_{i,j}$. Finally, $S_3 = \sum_{j=1}^{F}\sum_{i=j+1}^{F} A_{i,j} = \sum_{i=1}^{F}\sum_{j=i+1}^{F} A_{j,i}$ by exchanging i and j. Thus, the numerator can be rewritten as

$$\begin{aligned}&\sum_{i=1}^{F}\sum_{j=i+1}^{F}(A_{i,j}+A_{j,i}) = \\ &\sum_{i=1}^{F}\sum_{j=i+1}^{F}\frac{(\theta-1)(\gamma_j(P)-\gamma_i(P))^2}{(1+\gamma_i(P))(1+\theta\gamma_j(P))(1+\gamma_j(P))(1+\theta\gamma_i(P))}.\end{aligned} \tag{11}$$

Since the denominator in (10) is always positive and the numerator is also positive if $\theta \geq 1$ ($P \leq P_{ref}$), we have $\beta(P) \geq \frac{P}{P_{ref}}\beta(P_{ref})$. Otherwise, $\beta(P) < \frac{P}{P_{ref}}\beta(P_{ref})$.

Appendix B
Proof of Theorem 2

First of all, we prove the behavior of $\beta(P)$ in two extreme cases. As P goes to zero, $\beta(P)$ converges to $m(P)$ since

$$\begin{aligned}\lim_{P\to 0}\frac{\beta(P)}{m(P)} &= \lim_{\gamma_l(P)\to 0}\frac{\frac{1}{F}\sum_{l=1}^{F}\frac{\gamma_l(P)}{1+\gamma_l(P)}}{\frac{1}{F}\sum_{l=1}^{F}\frac{1}{1+\gamma_l(P)}}\frac{1}{\frac{1}{F}\sum_{l=1}^{F}\gamma_l(P)}\\ &= \lim_{\gamma_l(P)\to 0}\frac{\sum_{l=1}^{F}\gamma_l(P)}{\sum_{l=1}^{F}\gamma_l(P)} = 1.\end{aligned} \tag{12}$$

As P goes to infinity, $\beta(P)$ converges to $\tilde{m}(P)$ since

$$\begin{aligned}\lim_{P\to\infty}\frac{\beta(P)}{\tilde{m}(P)} &= \lim_{\gamma_l(P)\to\infty}\frac{\frac{1}{F}\sum_{l=1}^{F}\frac{\gamma_l(P)}{1+\gamma_l(P)}}{\frac{1}{F}\sum_{l=1}^{F}\frac{1}{1+\gamma_l(P)}}\frac{1}{F}\sum_{l=1}^{F}\frac{1}{\gamma_l(P)}\\ &= \lim_{\gamma_l(P)\to\infty}\frac{\sum_{l=1}^{F}\frac{1}{\gamma_l(P)}}{\sum_{l=1}^{F}\frac{1}{\gamma_l(P)}} = 1.\end{aligned} \tag{13}$$

These observations can be predicted from the properties of MMSE equalization coefficients $g_l = \sqrt{P}h_l^*/(P|h_l|^2+\sigma_0^2)$ in the two extreme cases. If P goes to zero, the MMSE equalization becomes maximal ratio combining as $g_l = \sqrt{P}h_l^*/\sigma_0^2$. Then, the MMSEC SNR becomes the arithmetic mean of subcarrier SNRs. On the other hand, the MMSE equalization becomes orthogonal combining such that $g_l = 1/(\sqrt{P}h_l)$ if P goes to infinity. Thus, the MMSEC SNR becomes the harmonic mean of subcarrier SNRs.

We now prove (7) by mathematical induction. For the notational simplicity, we rewrite (7) as $m^{(F)} = \sum_{l=1}^{F}\gamma_l$, $\tilde{m}^{(F)} = 1/\chi^{(F)}$ with $\chi^{(F)} = \sum_{l=1}^{F}\gamma_l^{-1}$, and $\beta^{(F)} = \frac{\eta^{(F)}}{1-\eta^{(F)}}$ with $\eta^{(F)} = \sum_{l=1}^{F}\frac{\gamma_l}{1+\gamma_l}$. If $F = 1$, (7) is true since $\tilde{m}^{(1)} = \beta^{(1)} = m^{(1)} = \gamma_1$. We assume that it is true for $F = i-1$. We then prove (7) for $F = i$ as follows.

We first prove the lower bound by showing that $\beta^{(i)} - \tilde{m}^{(i)} \geq 0$. To facilitate the proof, we rewrite

$$\beta^{(i)} - \tilde{m}^{(i)} = \frac{\chi^{(i)}\eta^{(i)}+\eta^{(i)}-1}{\chi^{(i)}(1-\eta^{(i)})} \triangleq \frac{\Lambda_{lo}}{\Delta_{lo}}, \tag{14}$$

where (a) $\Delta_{lo} = \chi^{(i)}(1-\eta^{(i)}) \geq 0$ since $\eta^{(i)} \leq 1$ and $\chi^{(i)} \geq 0$. In addition, we have

$$\begin{aligned}\Lambda_{lo} =& -1+\frac{i\gamma_i+1}{i^2(1+\gamma_i)}+\frac{i-1}{i^2}\frac{\eta^{(i-1)}}{\gamma_i}\\ &+\frac{(i-1)^2}{i^2}\chi^{(i-1)}\left(\eta^{(i-1)}+\frac{1}{i-1}\frac{\gamma_i}{1+\gamma_i}\right)\end{aligned} \tag{15}$$

since $\chi^{(i)} = \frac{i-1}{i}\chi^{(i-1)} + \frac{1}{i\gamma_i}$ and $\eta^{(i)} = \frac{i-1}{i}\eta^{(i-1)} + \frac{1}{i}\frac{\gamma_i}{1+\gamma_i}$. By using the fact that $\chi^{(i-1)} \geq \frac{\eta^{(i-1)}}{1-\eta^{(i-1)}}$, we obtain $\Lambda_{lo} \geq \frac{i-1}{i^2}\left(z+\frac{1}{z}-2\right)$, where $z = \frac{\eta^{(i-1)}(1+\gamma_i)}{\gamma_i}$. Since $z+\frac{1}{z} \geq 2$ for $z > 0$, we have (b) $\Lambda_{lo} \geq 0$. With (a) and (b), we prove that $\beta^{(i)} \geq \tilde{m}^{(i)}$. The upper bound is similarly proved by showing that $m^{(i)} - \beta^{(i)} \geq 0$. Again, we rewrite

$$m^{(i)} - \beta^{(i)} = \frac{m^{(i)} - m^{(i)}\eta^{(i)} - \eta^{(i)}}{1-\eta^{(i)}} \triangleq \frac{\Lambda_{up}}{\Delta_{up}}, \tag{16}$$

where $\Delta_{up} = 1-\eta^{(i)}$ and

$$\begin{aligned}\Lambda_{up} =& \frac{(i-1)^2}{i^2}(1-\eta^{(i-1)})m^{(i-1)}\\ &+\frac{(i-1)}{i^2}\left((1-\eta^{(i-1)})+\frac{m^{(i-1)}i+\gamma_i}{1+\gamma_i}\right).\end{aligned} \tag{17}$$

Since $(1-\eta^{(i)})$ is nonnegative, $\Delta_{up} \geq 0$ and $\Lambda_{up} \geq 0$. Thus, we prove that $m^{(i)} \geq \beta^{(i)}$.

ACKNOWLEDGMENT

The authors wish to express their appreciation of the invaluably constructive suggestions and helpful comments from the Associate Editor and anonymous reviewers.

REFERENCES

[1] S. Chatterjee, W. A. C Fernando, and M. K. Wasantha, "Adaptive modulation based MC-CDMA systems for 4G wireless consumer applications," *IEEE Trans. Consumer Electron.*, vol. 49, no. 4, pp. 995-1003, Nov. 2003.

[2] D. S. Oh, D. Kim, and S. Hwang, "Introduction of 4G activities in Korea," *IST Mobile Summit*, Dresden, June 2005.

[3] "Air interface for fixed broadband wireless access systems: PHY and MAC layers for combined fixed and mobile operation in licensed bands," IEEE P802.16e-2005, Feb. 2006.

[4] 3GPP TR 25.814, "Physical layer aspects for evolved universal terrestrial radio access (UTRA)," 3GPP, vol. 7.1.0, Oct. 2006.

[5] M. Jiang and L. Hanzo, "Multiuser MIMO-OFDM for next-generation wireless systems," *Proc. IEEE*, vol. 95, no. 7, pp. 1430-1469, July 2007.

[6] D. Kivanc, G. Li, and H. Liu, "Computationally efficient bandwidth allocation and power control for OFDMA," *IEEE Trans. Wireless Commun.*, vol. 2, no. 6, pp. 1150-1158, Oct. 2003.

[7] E. S. Lo, P. W. C. Chan, V. K. N. Lau, R. S. Cheng, K. B. Letaief, R. D. Murch, and W. H. Mow, "Adaptive resource allocation and capacity comparison of downlink multiuser MIMO-MC-CDMA and MIMO-OFDMA," *IEEE Trans. Wireless Commun.*, vol. 6, no. 3, pp. 1083-1093, Mar. 2007.

[8] R. Kimura and F. Adachi, "Comparison of OFDM and multicode MC-CDMA in frequency selective fading channel," *IEE Electron. Lett.*, vol. 39, no. 3, pp. 317-318, Feb. 2003.

[9] K. S. Kim, Y. H. Kim, and J. Y. Ahn, "An efficient adaptive transmission technique for LDPC coded OFDM cellular systems using multiple antennas," *IEE Electron. Lett.*, vol. 40, no. 6, pp. 396-397, Mar. 2004.

[10] K. S. Kim, "Adaptive modulation and power allocation technique for LDPC-coded MIMO-OFDMA cellular systems," *IEICE Trans. Commun.*, vol. E88-B, no. 11, pp. 4410-4412, Nov. 2005.

[11] Y. W. Blankenship, P. J. Sartori, B. K. Classon, V. Desai, and K. L. Baum, "Link error prediction methods for multicarrier systems," in *Proc. IEEE Veh. Technol. Conf.*, vol. 6, pp. 4175-4179, Sept. 2004.

[12] J.-F. Helard, J.-Y. Baudais, and J. Citerne, "Linear MMSE detection technique for MC-CDMA," *IEE Electron. Lett.*, vol. 36, no. 7, pp. 665-666, Mar. 2000.

[13] S. Verdu, *Mulituser Detection.* Cambridge, UK: Cambridge University Press, 1998.

[14] D. Tse and P. Viswanath, *Fundamentals of Wirelesss Communication*. New York: Cambridge University Presss, 2005.

[15] Recommendation ITU-R M.1225, *Guidelines for evaluation of radio transmission technologies for IMT-2000*, 1997.